Environmental and Experimental Botany 228 (2024) 105987

Contents lists available at ScienceDirect

Environmental and Experimental Botany

journal homepage: www.elsevier.com/locate/envexpbot

Research paper

Physiological and proteomic responses of *Posidonia oceanica* to phytotoxins of invasive *Caulerpa* species

Daniela Oliva [a], Amalia Piro [a], Marianna Carbone [b], Ernesto Mollo [b], Manoj Kumar [c,d], Faustino Scarcelli [a], Dante Matteo Nisticò [a], Silvia Mazzuca [a,*]

[a] University of Calabria, Department of Chemistry and Chemical Technologies, Laboratory of Plant Biology and Plant Proteomics (Lab.Bio.Pro.Ve), 87036 Rende, Italy
[b] Institute of Biomolecular Chemistry, National Research Council of Italy, Pozzuoli, Naple 80078, Italy
[c] Climate Change Cluster, University of Technology Sydney, Ultimo, NSW 2007, Australia
[d] Central Queensland University, Gladstone Campus, School of Health, Medical and Applied Sciences, Coastal Marine Ecosystems Research Centre, Australia

ARTICLE INFO

Keywords:
allelochemical interaction
Caulerpa cylindracea
Caulerpa taxifolia
caulerpenyne
caulerpin
invasive seaweed
mesocosm trial
seagrass proteomics

ABSTRACT

The invasive green algae *Caulerpa taxifolia* (M. Vahl) C. Agardh, 1817 and *Caulerpa cylindracea* Sonder, 1845 are widely diffused in the Mediterranean Sea, where they compete for space with the endemic seagrass *Posidonia oceanica* (Linnaeus) Delile, 1813, a keystone species in Mediterranean marine biodiversity. The present study aims to explore the possible effects of bioactive metabolites from the invasive algae on the seagrass, which may imply an allelopathic action. In particular, the study focuses on the effects of the algal alkaloid caulerpin and the sesquiterpene caulerpenyne. Changes in leaf growth, chlorophyll content, and leaf protein expression of *P. oceanica* genets under treatments were evaluated after 28 days of cultivation in mesocosms. Caulerpenyne strongly inhibited the growth of adult leaves and the formation of new ones, while inducing the elongation of the intermediate leaves and increased total chlorophyll content; on the contrary, caulerpin did not significantly influence leaf growth and the formation of new ones. A total of 107 differentially accumulated proteins common to the two treatments were also identified using the proteomic approach. Both molecules induced cells to maintain homeostasis, enhancing the amino acid metabolism or fatty acid biosynthesis. Despite these disruptions, *P. oceanica* demonstrated a more efficient response to stress induced by caulerpin, stimulating the biosynthesis of essential amino acids to maintain cellular homeostasis and mitigate damage caused by reactive oxygen species (ROS). Overall, obtained results supports the possible role of caulerpenyne, and not caulerpin, as an effector in allelopathic interactions among invasive *Caulerpa* species and *P. oceanica* in the Mediterranean.

1. Introduction

The introduction of allochthonous species, whether intentional or accidental, poses a significant risk to ecosystems worldwide (Kolar and Lodge, 2001). These non-native species, when they become invasive, can disrupt the balance of ecosystems, leading to adverse impacts on biodiversity and ecosystem services (Streftaris, N. & Zenetos, et al., 2006). Current climate change and the rise in water temperatures had influenced the biology and survival of species, aiding their spread into new habitats. From bad to worse, invasive species lack natural predators or pathogens in their new environment and can proliferate rapidly, outcompeting native species and altering the ecosystem dynamics. These changes can have far-reaching consequences, affecting not only biodiversity but also ecosystem functions and services. Additionally, some introduced species may be toxic or harmful, posing risks not only to the environment but also to human health if they enter the food chain or directly affect human activities. In this context, the invasive success of the exotic green algae *Caulerpa taxifolia* and *Caulerpa cylindracea* in the Mediterranean can be attributed to their peculiar adaptability and invasiveness, including their high tolerance to nutrient and light stress (Meinesz et al., 1996; Chisholm et al., 1996; Delgado et al., 1996; Ceccherelli and Cinelli, 1999; Williams & Grosholsz, 2002; Ceccherelli et al, 2002). This adaptability allows them to establish and proliferate in new environments where native species may struggle, leading to their dominance and altering ecological dynamics. The mechanisms by which *C. taxifolia* and *C. cylindracea* influence native vegetation, particularly seagrasses, are not entirely understood; A previous study by Holmer et al. (2009) demonstrated that species from the *Caulerpa* genus modify

* Corresponding author.
E-mail address: silvia.mazzuca@unical.it (S. Mazzuca).

https://doi.org/10.1016/j.envexpbot.2024.105987
Received 1 August 2024; Received in revised form 6 September 2024; Accepted 23 September 2024
Available online 28 September 2024

sediment conditions by increasing organic matter, microbial activity, and sulfide levels, likely contributing to the decline of *Posidonia oceanica* as *Caulerpa* appears to thrive more effectively than the seagrasses in the altered environment (Zubia et al., 2020).

Two bioactive compounds belonging to the *Caulerpa* genus, well acknowledged in the literature, are excellent repellents for herbivores, the bisindole alkaloid Caulerpin, whose structure was first proposed in 1970 (Liu et al., 2012) and the sesquiterpene Caulerpenyne. Caulerpin is mostly biosynthesized by *C. cylindracea* and Caulerpenyne is the most abundant metabolites in *C. taxifolia*. These molecules, claimed as "alien metabolites" (Defranoux and Mollo, 2020; Mollo et al., 2015; 2023) have been demonstrated to possess a series of antibacterial properties and to be bioactive against human diseases (Sfecci et al., 2017). Therefore, environmental monitoring for the presence of *Caulerpa* species must consider the possibility of allelopathic interactions affecting native communities (Shea and Chesson, 2002; Simberloff et al., 2013).

Posidonia oceanica, the distinctive seagrass native to the Mediterranean, exhibits significant vulnerability to *Caulerpa* sp. However, the specific strategies employed for competition when in contact with either *C. cylindracea* or *C. taxifolia* are not thoroughly understood (Holmer et al., 2009). Over a decade of long-term monitoring has revealed that prolonged interaction with *C. taxifolia* has had a detrimental impact on the structure of *P. oceanica* meadows (Molenaar et al., 2009; Pergent et al., 2008). Conversely, *C. cylindracea* has demonstrated limited ability to penetrate healthy *P. oceanica* meadows (Bernardeau-Esteller et al., 2020).

The persistent inquiry surrounding the interaction between plants and algae remains unanswered, prompting various theories to emerge. One such hypothesis posits that algae might release allelopathic molecules, causing cytotoxic effects on the plant (Motmainna et al., 2023). Another theory suggests that the fragmentation of algal thalli results in sediment deposition, leading to the accumulation of bioactive metabolites. This, in turn, alters the microenvironment, creating unfavorable conditions for plant growth (Piazzi et al., 2005). It is essential to delve into this question to gain a comprehensive understanding.

Investigating the mechanism of competition is vital for unraveling the true invasive potential of algal species and comprehending the extent of disruption they can cause. This impact is not limited to native species alone but extends to the entire ecosystem they inhabit. In this study, we conducted a manipulative laboratory experiment where purified caulerpin and caulerpenyne were introduced to the rhizomes of *P. oceanica* cuttings within mesocosms over a 28-day period. The primary objectives were to confirm the translocation of these molecules within the tissue, reaching the leaf blades, and to assess their potential effects in that region. Leaf growth, chlorophyll content, and differential protein expression were assessed to evaluate the impact of these deliberate treatments on plant growth and metabolism.

2. Materials and methods

2.1. Extraction and purification of the algal metabolites

To obtain the necessary quantity of caulerpenyne (CYN) for the subsequent treatment of *P. oceanica* in mesocosm conditions, 450 g (wet weight) of *Caulerpa prolifera* (Forsskål) J.V.Lamouroux, 1809, the native Mediterranean alga from which CYN was originally isolated (Amico et al., 1978), was exhaustively extracted with acetone (Sigma-Aldrich; 500 ml × 3 times) through homogenization and sonication in a ultrasonic bath (FALC ultrasonic bath, KHz 50), following the method described in Carbone et al. (2008). The acetone extract was then evaporated under reduced pressure by using a rotary evaporator (Büchi R-210), and the aqueous residual was further extracted with diethyl ether (Sigma-Aldrich; 500 ml × 4 times in a separation funnel) to obtain 4 g of crude diethyl ether extract. Subsequently, a portion (1 g) of the diethyl ether extract was subjected to gel filtration column chromatography by using Sephadex LH-20 (GE Healthcare) to give a caulerpenyne-containing fraction (320.0 mg), which was further purified by silica gel column chromatography (Merck Kieselgel 60 powder) using a petroleum ether/diethyl ether gradient. Pure CYN (100 mg), identified by comparing ^{1}H NMR data with literature values (Amico et al., 1978) was eluted with petroleum ether/diethyl 8:2. The NMR spectrum of CYN (Fig. 1a) was recorded using a 400 MHz Bruker Avance III HD spectrometer equipped with a CryoProbe Prodigy.

Similarly, to obtain pure caulerpin (CAU), a sample of *C. cylindracea* (1200 g wet weight) was exhaustively extracted with acetone (Sigma-Aldrich; 650 ml × 6 times), employing homogenization and sonication as described above for the extraction of *C. prolifera*. The subsequent extraction of the aqueous residual with diethyl ether (Sigma-Aldrich; 500 ml × 4 times in a separation funnel) afforded 3 g of crude diethyl ether extract, a portion of which (1.6 g) was then subjected to gel filtration column chromatography by using Sephadex LH-20 (GE Healthcare), resulting in the isolation of a fraction that was determined to contain only the alkaloid CAU (70 mg, red/orange prisms), identified by comparing its ^{1}H NMR data (Fig. 1b) with literature values (Anjaneyulu et al., 1991; Chay et al., 2014). The NMR spectrum of CAU was recorded using a 400 MHz Bruker Avance III HD spectrometer equipped with a CryoProbe Prodigy.

2.2. Collection of plants, mesocosm cultivation and treatments

The plants were sampled in November 2022 along the Calabria Thyrrenian coast (South Italy) from the site at Fondali Capo Vaticano (38°39'47" N; 15°50'38" E) where there have been no reports of *C. cylindracea* or *C. taxifolia* occurrence (Cantasano et al., 2017); this was essential to ensure the selection of *P. oceanica* genotypes that had not encountered the invasive algae before. Plants were collected at the same depth by scuba diving; each sample (genet), consisted of a plagiotropic rhizome with four ramets (Fig. 2a). Upon returning to the laboratory, to prevent infections, each rhizome's cut zone was safeguarded with a silicon cup filled with sterile seawater (Mazzuca et al. 2009). This approach allowed us to supply the molecules directly into the cut zone of rhizomes, facilitating systemic treatment (Fig. 2a). Each shoot consisted in adult, intermediate, and juvenile leaves (Fig. 2b). For the experimental trial, two solutions were prepared, (i) 25 μM CAU and (ii) 25 μM CYN, each dissolved in the seawater added with 1 % of dimethyl sulfoxide as vehicle (DMSO) to facilitate solubilization of both hydrophobic molecule; genets treated with seawater added with 1 % of DMSO were used as reference. A total of 18 genets, with six for each treatment, were utilized. Genets were placed in mesocosms each of 130 liter capacity, 21 ± 0.1 °C (thermal controller TECO TK 500 H, 4.0 SCUBLA S.r.l), pH 8.1, and 36 ± 0.5 ppm salinity, recirculation pump equipped with Backpack mechanical/biological filter (Internal skimmer), 12/12 h light/dark cycle under white/blue light LED lighting system. After a 28-day period, dead leaves and freshly emerged ones were tallied in all genets. Leaf growth rate was assessed by measuring the increase in leaf length relative to the reference (Fig. 2c), cleaned from epiphytes, swiftly washed in distilled water, frozen in liquid nitrogen, and subsequently stored at −80 °C for biochemical and molecular analyses.

2.3. Chlorophyll extraction

Chlorophyll was extracted from leaves of five biological replicates for the reference and each treatment. Leaf tissues (1.0 g) were finely ground into powder using a mortar and pestle with liquid nitrogen. Subsequently, 5 ml of 80 % cold acetone was added to the tissue powder and incubated at 4 °C for 3 hours-. After incubation, the mixture was centrifuged at 6000 g for 15 min. Following centrifugation, 1 ml of the supernatant was transferred to a quartz cuvette, and the absorbances at 663 nm and 645 nm were measured using the Jenway 7310 Advanced Visible Spectrophotometer (Cole-Parmer Instrument Co. Europe, UK). The concentrations of chlorophylls *a* and *b*, as well as total chlorophyll, were determined using the equations provided by Hiscox et al. (1979).

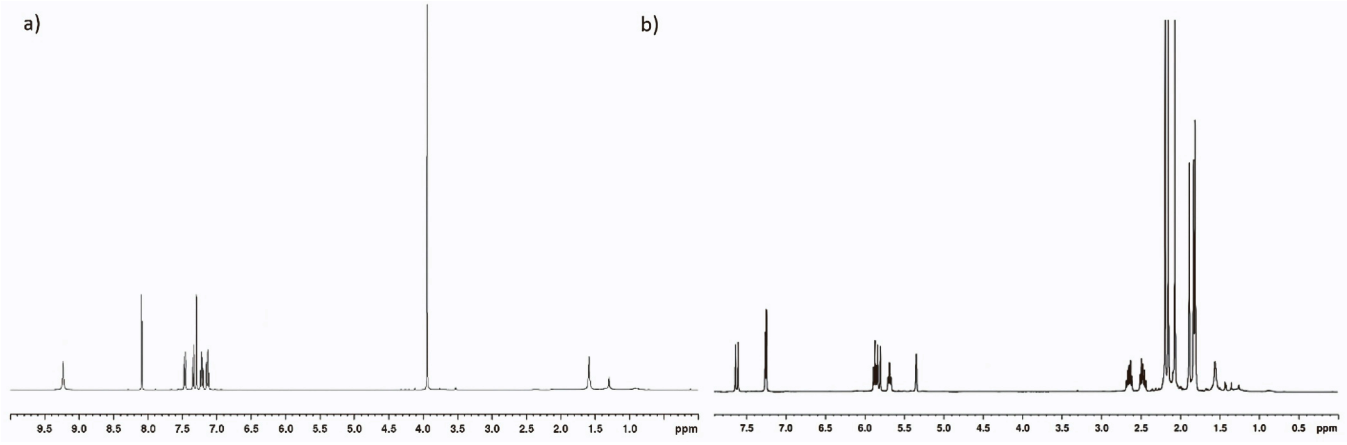

Fig. 1. a) ^{1}H NMR spectrum of caulerpin (CAU); b) ^{1}H NMR spectrum of caleurpenyne (CYN).

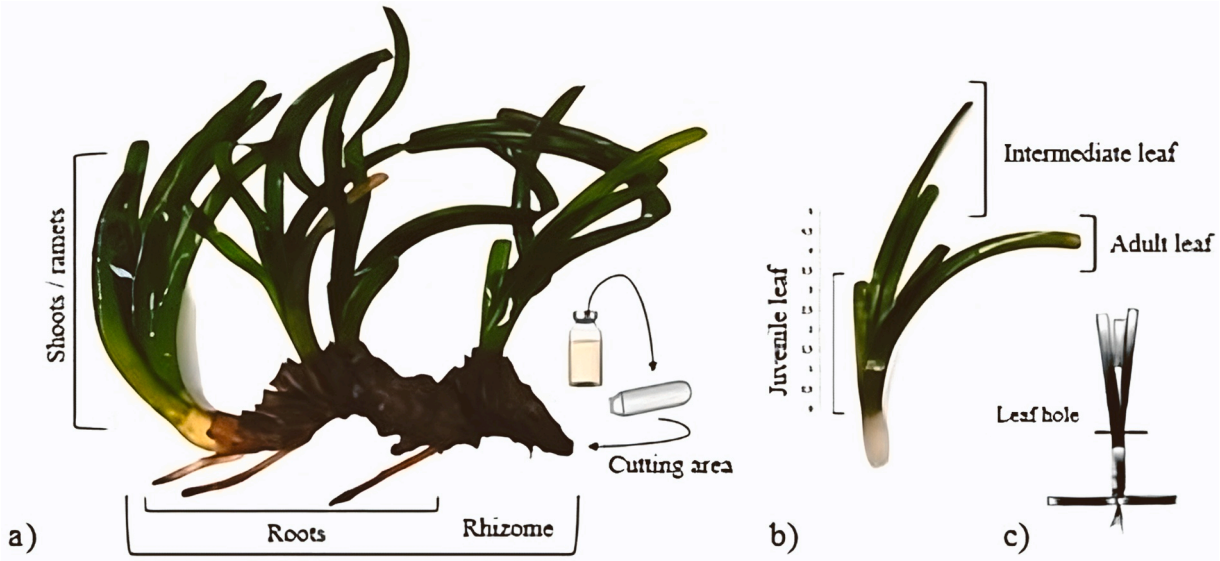

Fig. 2. a) Genet of Posidonia oceanica with four ramets and roots distributed along a rhizome; b) Shoot exhibiting leaves at different developmental stages, comprising of adult, intermediate (in differentiation stage) and juvenile (<5 cm in length); c) reference point marked up to its leaf base; following a 28-day interval, the distance between the marked reference point and the leaf base was quantified (Zieman, 1974; Buia et al, 1992).

2.4. Leaf protein extraction and purification

Protein extraction from leaves of six biological replicates for the reference and treatments followed a modified methodology as described in Piro et al. (2020). Frozen leaves (1 g) were ground into a fine tissue powder using a mortar. The powder was then divided into 2 ml vials for protein extraction and precipitation. Approximately five volumes of 20 % trichloroacetic acid (TCA) in water were added to each vial, followed by centrifugation at 14,000 g for 5 min at 4 °C. The resulting pellet, containing the precipitated proteins, was washed in 80 % acetone and air dried in a vacuum centrifuge at room temperature for 1 hour. For protein purification, 0.1 g of the pellet was dissolved in 0.8 ml of phenol (buffered with Tris-HCl, pH 8.0, Sigma, St. Louis, MO, USA) and 0.8 ml of SDS buffer (30 % sucrose, 2 % SDS, 0.1 M Tris-HCl, pH 8.0, 5 % 2-mercaptoethanol) in 2 ml vials. After centrifugation at 14,000 g, five volumes of 0.1 M ammonium acetate in cold methanol were added to the phenolic phase, and the mixture was stored at −20 °C for 30 min. Proteins were then collected by centrifugation at 14,000 g for 5 minutes and washed in 0.1 M ammonium acetate/methanol and 80 % acetone. The final pellet, containing purified proteins, was air dried at room temperature and dissolved to a final concentration using Laemmli 1D electrophoresis buffer (Laemli, 1970). Protein quantification was performed by measuring absorbance at 595 nm using the Bradford assay (Bradford, 1976). Protein yield was calculated as mg of protein per g fresh tissue weight in three biological replicates for each sample. The relative abundances of proteins were calculated as the mean value ± standard error (n = 3). Pairwise comparisons between samples were conducted using a student t-test, with p-levels of 0.05 used as the threshold for statistical significance unless otherwise noted.

2.5. SDS-PAGE electrophoresis of proteins, in gel digestion and mass spectrometry

Leaf protein separation was accomplished using a modified short-term electrophoresis protocol, optimizing the process by concentrating each replicate into a shorter lane compared to conventional electrophoresis methods (Oliva et al., 2023). In this procedure, protein samples (20 μg) were loaded onto 12 % acrylamide/bisacrylamide gels and electrophoresed for 30 minutes under a constant power of 200 V at 120 mA. Subsequently, the gels were stained overnight in Coomassie Blue solution. Digitized SDS-PAGE images were analyzed using 1-D Quantitative Analysis Software (Bio-Rad, Berkeley, USA) to measure

the band density in each lane across all biological replicates. The stained bands were then manually excised from the gels, destained in a solution of 50 mM ammonium bicarbonate and acetonitrile (ACN) (1:1 v/v), and subjected to reduction/alkylation steps using 55 mM iodacetamide at room temperature for 30 min in the dark, and DTT at 56 °C for 20 min, following the protocol by Shevchenko et al. (2006). The reduced and alkylated gel slices were further processed for protein digestion in the gel using 0.02 μg/μl trypsin dissolved in 25 mM AmBic (Promega, Madison WI, USA) overnight at 37 °C, with additional ammonium bicarbonate buffer to cover the gel matrix. The resulting tryptic peptides were extracted with 5 % formic acid (FA) in water, washed in acetonitrile and ammonium bicarbonate (50 mM), and dried. Subsequently, the tryptic peptides were dissolved in 20 μL of 8 % formic acid in water and immediately prepared for mass spectrometry analysis.

2.6. Mass spectrometric analysis

LC−MS/MS analysis was performed using an EASY-LC 1000 system (Thermo Fisher Scientific, Denmark) coupled to a hybrid quadrupole/Orbitrap Q-Exactive mass spectrometer (Thermo Fisher Scientific, Germany). An in-house-made analytical column (14 cm long, with an inner diameter of 75 μm) packed with 3 μm C18 silica particles (Dr. Maisch, Entringen, Germany) was utilized. Prior to analysis, samples were diluted 5-fold in 0.1 % formic acid, and 2 μL of the resulting peptide mix was injected for LC-MS/MS analysis. The mobile phase composition for liquid chromatography (LC) consisted of 2 % acetonitrile, 0.1 % formic acid for mobile phase A, and 80 % acetonitrile, 0.1 % formic acid for mobile phase B. The LC gradient initiated with 0 % mobile phase B, reaching 3 % B within 1 second, increasing to 40 % B over 120 min, followed by a 100 % B phase for an additional 8 min. After 5 min at 100 % B, the mobile phase composition returned to 0 % B in 2 minutes, resulting in a total run time of 135 minutes at a flow rate of 230 nL/min. The column effluent underwent nano-electrospray ionization (1600 V of nESI potential), and charged species were detected by the Q-Exactive hybrid mass spectrometer operating in positive ion mode. A full MS scan was acquired in the Orbitrap analyzer with a resolution of 70,000, covering a mass-to-charge ratio (m/z) range of 350−1800, and a target AGC value of 1.00 × 106. Data-dependent MS/MS acquisition (DDA) was performed by selecting the 12 most abundant peaks with more than two charges after each full scan analysis using the top 12 method. Precursor ions were fragmented by high-energy collisional dissociation (HCD) with a normalized collision energy of 25 %. MS/MS analysis was carried out in the Orbitrap analyzer at a resolution of 35,000, with a target AGC value of 1.0 × 105, an intensity threshold of 5.0 × 10 4, and an isolation window of 1.6 m/z. A maximum injection time of 50 ms was set for the full MS scan event, while tandem MS/MS scans had a maximum injection time of 120 ms. The dynamic exclusion time was set to 30 seconds.

2.7. Bioinformatic analysis and proteins identification

From the MS/MS spectra, protein inference and validation were performed with the Peaks Studio software (Bioinformatic Solution Inc, Waterloo, Canada). MS/MS spectra were extracted from raw data by accepting one minimum sequence of eight amino acids and fusion scans with the same precursor within one mass window of ± 0.4 m/z, over a time interval of ± 30 s. The key parameters of research are Scored Peak Intensity, (SPI) ≥ 50 %, precursor mass tolerance of ± 10 ppm and mass tolerance of product ions of ± 20 ppm. The carbamidomethylation of cysteine was fixed as a modification and trypsin was selected as the enzyme for the digestion, accepting two missing cleavages per peptide. The Automatic thresholds were used for peptide identification in the software Peaks. Generally, peptide probabilities are evaluated using a Bayesian approach for the estimation of the local FDR (LFDR) up to a value of 1 %. The peptide sequences using Peaks Studio software, were interfaced with both the database of proteins deduced from generalist protein sequences of *Zostera marina* deposited in the NCBI database (downloaded in November 2023) and in the bank UniProt data (downloaded in November 2023).The statistical gene enrichment test was carried out by using KEGG BlastKOALA (https://www.kegg.jp/blastkoala/; Kanehisa et al., 2016) the relative fold change of each GO term has been represented for "Biological process" categories Detailed peptide-to-protein assignments, along with relevant statistical parameters, are provided in Supplementary Tables 1.

2.8. Statistics analysis

Comparison of differences among groups of values for phenology and photosynthetic pigment, were analyzed using t-test with p <0.05 threshold for statistical significance. All the statistical analyses were performed using Excel XLSTAT (©Addinsoft, Paris, France, released at 2022.6.1.1187). Significance was defined as $p \leq 0.05$. For the proteomics results, comparison of differences among the groups was carried out using the Differentially Expression and Heat map tools available at Excel XLSTAT. Bonferroni test was used to test the assumption of homogeneity of variances. Threshold for significance was $p \leq 0.05$.

3. Results

3.1. Leaf renewal, leaf growth rate and chlorophyll content after CAU e CYN treatments

Ramets treated with CYN exhibited a moderate leaf mortality of adult leaves and a hindrance in new leaf emergence (42 %). However, it stimulated the growth and number of intermediate leaves (38 %), surpassing the reference. Consequently, the ramets experienced a substantial increase in the percentage of intermediate leaves compared to the reference samples. In contrast, CAU did not significantly alter the leaf composition in the ramets compared to the reference counterparts, although a modest decrease in juvenile leaves was observed. Therefore, following CAU treatment, the ramets exhibited an equal distribution of adult and intermediate leaves (Fig. 3).

In Fig. 4, the leaf growth rate after 28 days of cultivation is depicted. Both CAU and CYN significantly decreased the growth rate of surviving adult leaves, particularly in the CYN treatment. Moreover, the growth rate of intermediate leaves was also negatively affected with major effects under CAU treatment. Regarding adult leaves, in the reference box plot, the interquartile range (IQR), which encompasses the middle 50 % of the data, are comprised in a short range from 1.2 to 1.7 cm with few outliers values. CYN treatment lowered the tendency and the IQR settling the values below 0.5 cm with many values around zero; few outliers were also displayed. Box plot related to CAU treatment indicated a IQR range slightly higher than that recorded in the CYN treatment, with a comparable mean value (Fig. 4).

Intermediate leaves grew faster than adult ones, as expected. In the reference samples, the IQR spanned from 4 to 5.5 cm, while it notably lowered ranged from 3 to 4.5 cm in CYN-treated ramets. The presence of numerous outliers suggested a heterogeneous growth rate among these types of leaves under CYN treatment. CAU treatment further reduced the minimum value of IQR to 2 cm with an individual outliners around 1.0 cm.

Chlorophyll *a* and *b* displayed notable variations in leaves exclusively following CAU treatment. The interquartile range (IQR) value groups spanned from minimum to maximum values, which were lower than those in the reference group, and the mean value was at its lowest in the CAU treatment (Fig. 5). It is crucial to highlight that the Chl*a*/Chl*b* ratio remained unchanged in the treated samples compared to the reference samples.

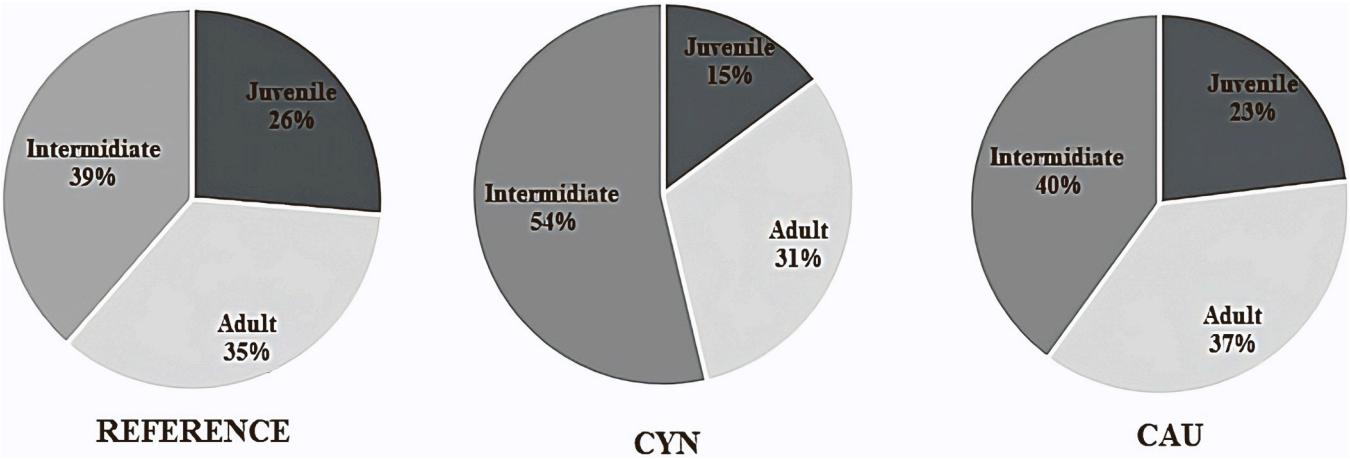

Fig. 3. Percentages of adult, intermediate and juvenile leaves in the ramets assessed after a 28-day period among reference genets, CYN and CAU treated *P. oceanica* genets.

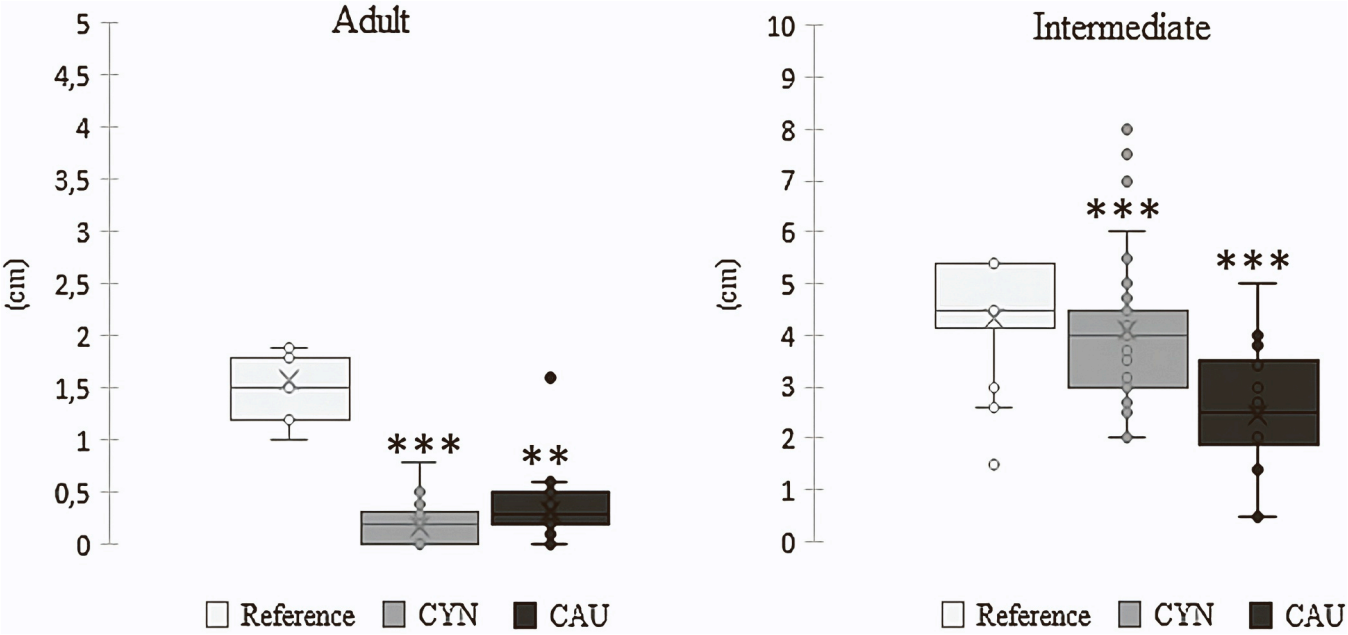

Fig. 4. Leaf growth rate of adult and intermediate leaves along the rhizome of P. oceanica after 28-days cultivation in reference genets and in those treated with 25 μM CAU and 25 μM CYN. Data represented as standard deviation (SD) and significance at $^{**}p<0.001$; $^{***}p<0.0001$ (student t test). n=18 genets each treatment; n=6 leaves each genet.

3.2. Quantitative analysis of leaf proteins of Posidonia oceanica treated with CAU and CYN

Quantitative proteomic analysis revealed the differential expression of 107 unique proteins varied in leaves following the CAU and CYN treatments (Supplementary Tables 1). To explore the metabolic pathways associated with these differentially accumulated proteins (DAPs), an enrichment analysis using KEGG BlastKOALA was performed, which identified functional categories detailed in Fig. 6. In the CAU treatment, ramets exhibited 52 DAPs, with 48 (93 %) mapped to 13 pathways in the KEGG database. Most of these proteins were involved in carbohydrate metabolism (30 %), followed by genetic information (20 %), energy metabolism (10 %), environmental information processing (10 %), and genetic information processing (10 %). In the CYN, treatment, 55 (DAPs) were detected, with 52 of them categorized into 14 pathways. Carbohydrate metabolism (40 %), genetic information (18 %), energy metabolism (10 %), and environmental information processing (10 %) were among the most prevalent pathways.

3.3. Differentially accumulated proteins (DAPs) identified in ramets treated with CAU and CYN

Heat maps depicting unsupervised clustering of samples and proteins based on their abundance and similarities in CAU and CYN treated genets, in comparison with reference samples, are illustrated in Fig. 7(a, b). Samples and proteins were clustered using correlation distance and hierarchical agglomerative clustering, with colors scaled per row. Interestingly, the patterns of accumulated and depleted proteins among the biological replicates showed significant inversion following the CAU and CYN treatments.

DAPs were categorized into various classes according to their molecular functions, biological processes, and cellular components. Protein classes that were overrepresented during CAU and CYN treatments are depicted in Fig. 7. As evident from the data, treatments resulted in the

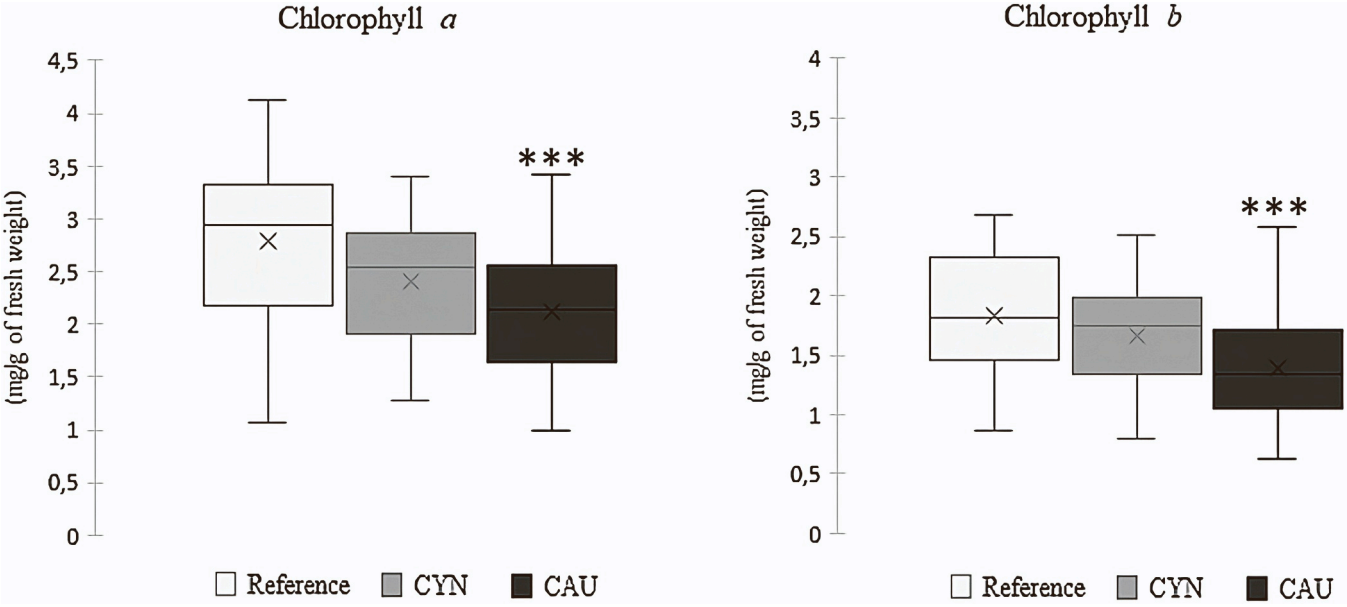

Fig. 5. Chl *a* and Chl *b* content in leaves from *P. oceanica* ramets after 28-days cultivation in reference, 25 μM CAU and 25 μ M CYN treated genets. Data represented as standard deviation (SD) and t-test student (***$p<0.0001$). n= -18 genets each treatment; n = -6 measurements each genet.

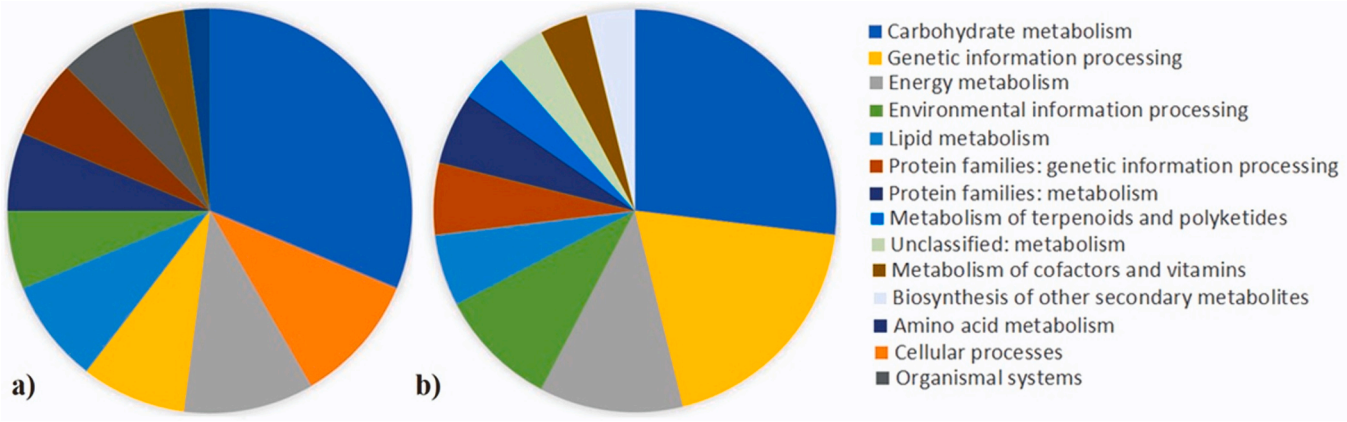

Fig. 6. Graphical view of metabolic pathways enriched following the treatment with a) 25 μM CAU and b) 25 μM CYN. Analyses performed with KEGG BlastKOALA on proteomic data from genets of *Posidonia oceanica* after 28-days cultivation.

enrichment of six protein class categories. In both treatments, the most prominent category was metabolites interconversion enzymes, followed by transferases (17 %) in CAU and oxidoreductases (17,5 %) in CYN. Additional classes enriched by treatments were lyases, kinases, dehydrogenase, actin and actin related proteins (Fig. 8).

After deciphering the biological processes (evaluated by their GO terms) of accumulated or depleted proteins in shoots treated with CAU, it was observed that the main depleted protein was involved in the transcription process (Table 1).

Remarkably, the level of TFIIS central domain-containing protein was quite hundred-fold lower compared to the reference samples. Additionally, CAU exerted a strong repressive effect on glycolytic process by the depletion of key enzyme Glyceraldehyde-3-phosphate dehydrogenase; malate dehydrogenase, phosphoenolpyruvate carboxylase, phosphopyruvate hydratase were also affected, suggesting an overall depletion of carbon metabolism. T-complex protein 1 subunit eta acting in protein folding, proteolysis with the RHOMBOID-like protein, three enzymes involved in protein translation were depleted. Several proteins associated with the stress response pathway underwent depletion under CAU treatment. Specifically, Serine hydroxymethyltransferase, Naringenin-chalcone synthase, and Phenylalanine ammonia-lyase reduced under the treatment. Moreover, CAU significantly depleted two Actin proteins, a Calcium lipid binding protein, Ras-related protein RABB1c and Coatomer subunit alpha linked to the intracellular vesicle transport. Histones H4 and H2B were depleted as also the nucleoside-diphosphate kinase, indicating chromatin structural rearrangements. Finally, photosynthesis was also affected with the Photosystem I reaction center and 7-hydroxymethyl chlorophyll a reductase 4-fold decreased in respect to the references. (Table1).

CAU treatment strongly induced the accumulation of proteins involve in aminoacid metabolism such as glutamine, methionine, cysteine, glycine and serine biosynthesis. Notably, Phosphoserine aminotransferase belong to the serine biosynthesis accumulated to xy fold by the CAU treatment. Further, Glycolytic enzymes (including Fructose-bisphosphate aldolase, Phosphoglycerate kinase) and tricarboxylic acid cycle enzymes namely Succinate dehydrogenase, ATP citrate synthase together with Phosphoribulokinase belonging the pentose-phosphate cycle accumulated were accumulated. Regarding cell organelles, vacuolar metabolism seemed to be affected most; the H (+)-exporting diphosphatase involved in the tonoplast membrane

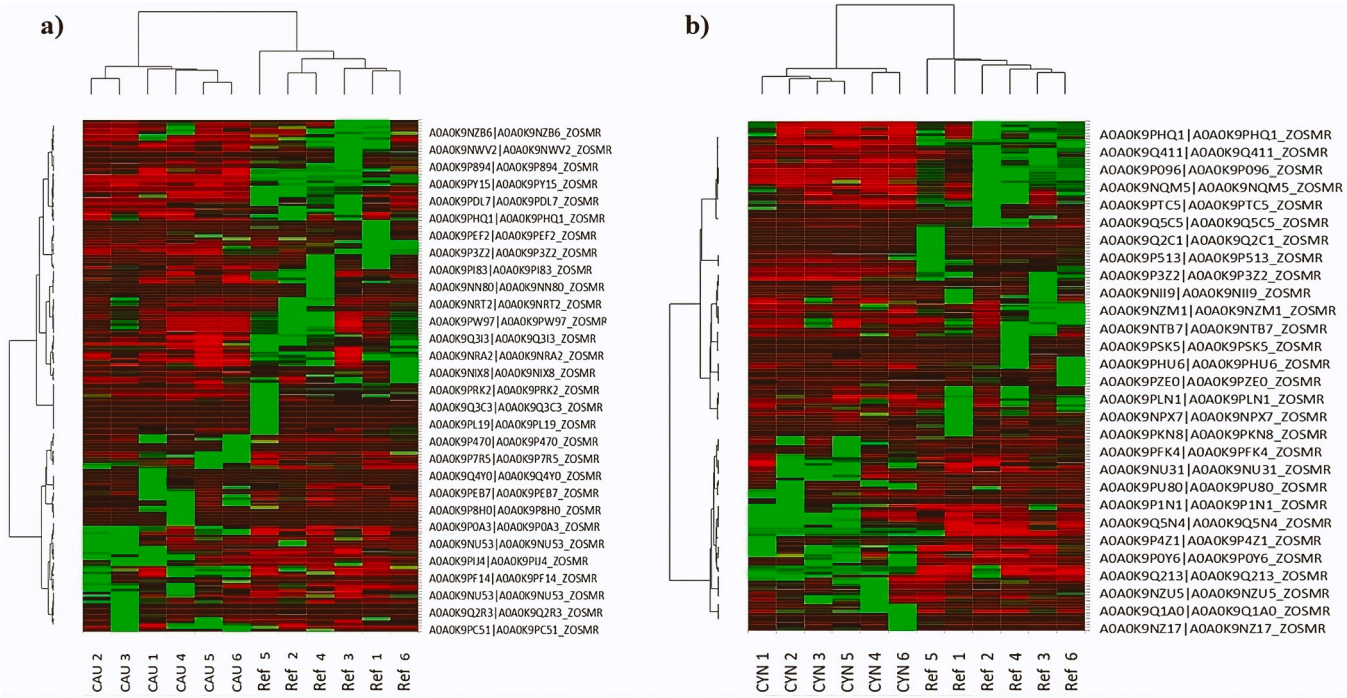

Fig. 7. Heat maps of proteins differentially accumulates after 28-days cultivation in leaves treated with CAU (a) and CYN (b). Protein expression values normalized to Log_2, and cluster analysis performed using fold change levels of proteins. The color code panels on the right indicate the described preferential expression of a protein. (XLSTAT 2022.6.1.1187 - Differential expression tool). The details of the analysis shown in the Supplementary Tables 1.

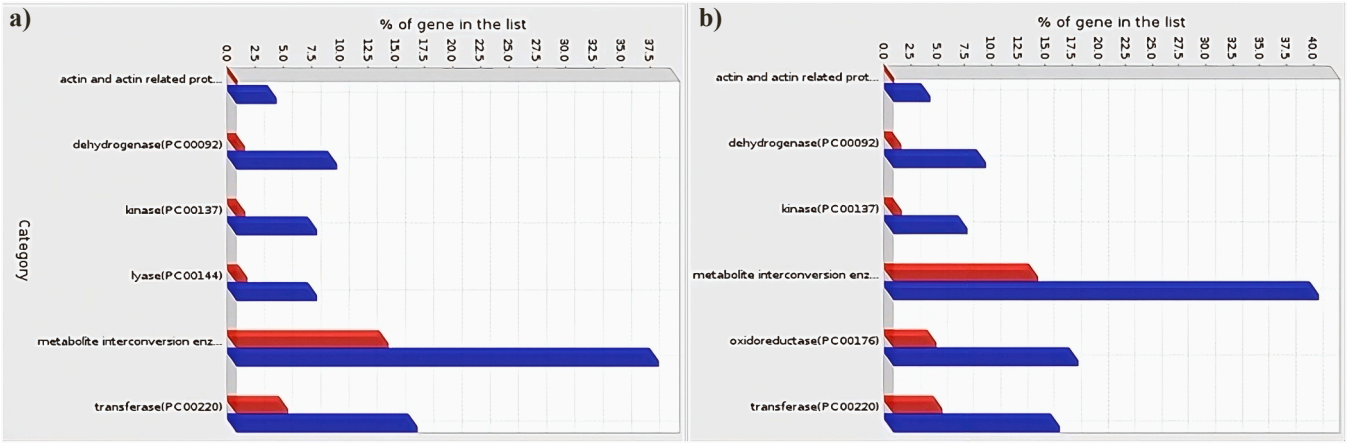

Fig. 8. Protein class enrichment in a) CAU and b) CYN treatments. Analyses were made by Panther™ (v. 14.0) Classification System tool (Mi et al., 2019). The reference protein class of *Zostera marina* (red boxes), and enriched protein class in *P. oceanica* (blue boxes) have been reported.

transport and vacuolar acidification was induced. Increased expression of Actin-depolymerizing factor 4 and enzymes associated with endoplasmic reticulum network organization suggest a restructuring of the cytoskeleton-dependent cellular trafficking pathways. Chlorophyll *a-b* binding protein and NmrA family protein involved in the photosystem II assembly were 4-fold accumulated.

CYN treatment affected the nuclear activities with a significant reduction in the levels of the TFIIS central domain-containing protein, which plays a crucial role in the transcriptional activity at the nuclear level of DNA templates, and of the Histone H2B. Carbohydrate metabolism strongly depleted; many enzymes belonging glycolysis such as Glyceraldehyde-3-phosphate dehydrogenase, Fructose-bisphosphate aldolase, Pyruvate kinase, Fructose-bisphosphate aldolase, transketolase, and Pantothenate kinase 2 depleted from 8- to 4-fold changes. Photosynthesis was negatively impacted with depletion in proteins including Chlorophyll a-b binding protein, Ferredoxin–NADP reductase, and DUF642 domain-containing protein, involved in photosynthetic light reactions. Additionally, glucose biosynthesis diminished due to the depletion of the RuBisCO large subunit-binding protein, responsible for assembling subunits (Table 2).

CYN resulted in the accumulation of proteins included Uridine kinase, an enzyme involved in the pyrimidine biosynthetic pathway, the Pleiotropic drug resistance protein responsible for abscissic acid transport, and the DCD domain-containing protein associated with the stress response of the endoplasmic reticulum. Further, ER to Golgi vesicle-mediated transport was promoted by CYN. CYN significantly affected the cytoskeleton by upregulating diverse actin proteins including actin-11 and actin-85 (accumulated to 4–8 folds). In addition to the cytoskeleton rearrangement, vacuolar V-type proton ATPase, linked to vacuole enlargement and cell growth were found upregulated. Stress

Table 1
Proteins that showed high variations in expression in leaves after the caulerpin (CAU) treatment are reported. The accession number, protein name, associated GO biological process, fold change (FC) expressed as Log_2 compared to reference, and statistical significance are provided.

Accession	Protein names	Biological Process	FC (Log_2)†	T-test *p*value*
A0A0K9NWS1	Phosphoserine aminotransferase	L-serine biosynthetic process	24.00	0.038
A0A0K9PUR8	Fructose-bisphosphate aldolase	glycolysis/gluconeogenesis	5.80	0.013
A0A0K9NZ17	Phosphoribulokinase	reductive pentose-phosphate cycle	2.90	0.049
A0A0K9NU31	Succinate dehydrogenase	tricarboxylic acid cycle	2.50	0.044
A0A0K9PU80	Glutamine synthetase	glutamine biosynthetic process	2.10	0.034
A0A0K9P513	Phosphoglycerate kinase	glycolysis/gluconeogenesis	2.00	0.012
A0A0K9P8U9	Chlorophyll a-b binding protein	photosynthesis	1.80	0.025
A0A0K9Q3W6	Actin-depolymerizing factor 4	actin filament depolymerization	1.70	0.004
A0A0K9NXT1	NmrA family protein	photosystem II assembly	1.60	0.042
A0A0K9NSU9	V-type proton ATPase proteolipid subunit	vacuolar acidification	1.50	0.003
A0A0K9P0X4	26S protease regulatory subunit	ubiquitin-dependent ERAD pathway	1.30	0.04
A0A0K9NMF8	Alcohol dehydrogenase-like protein	cellular response to hypoxia	1.30	0.02
A0A0K9PL77	Polyadenylate-binding protein	regulation of translation	1.30	0.035
A0A0K9P0A3	ATP citrate synthase	tricarboxylic acid cycle	1.20	0.008
A0A0K9Q5Y8	homocysteine S-methyltransferase	methionine biosynthetic process	1.20	0.019
A0A0K9P660	peptidylprolyl isomerase	cysteine biosynthetic process	1.20	0.038
A0A0K9NUP3	Serine hydroxymethyltransferase	glycine biosynthetic process from serine	1.10	0.017
A0A0K9P513	Phosphoglycerate kinase	glycolytic process	1.10	0.043
A0A0K9Q5S7	RNA helicase	translational	1.10	0.009
A0A0K9PRU0	H(+)-exporting diphosphatase	vacuolar acidification	1.10	0.035
A0A0K9P9B7	Protein lunapark	ER tubular network organization	−1.00	0.027
A0A0K9PCX9	Putative Cytochrome C1	mitochondrial electron transport	−1.00	0.006
A0A0K9Q4D0	Phenylalanine ammonia-lyase	cinnamic acid biosynthetic process	−1.00	0.038
A0A0K9NRA2	Histone H4	nucleosome assembly	−1.00	0.012
A0A0K9P3Z2	ATP-dependent 6-phosphofructokinase	fructose 6-phosphate metabolic process	−1.00	0.011
A0A0K9P1N6	Histone H2B	nucleosome assembly	−1.10	0.026
A0A0K9NJK7	phosphopyruvate hydratase	glycolytic process	−1.10	0.017
A0A0K9NRA2	Histone H4	nucleosome assembly	−1.10	0.023
A0A0K9NZB6	RHOMBOID-like protein	proteolysis	−1.10	0.038
A0A0K9Q3S1	nucleoside-diphosphate kinase	UTP biosynthetic process	−1.20	0.019
A0A0K9Q587	Ras-related protein RABB1c	vesicle-mediated transport	−1.20	0.044
A0A0K9PTC2	Coatomer subunit alpha	ER to Golgi vesicle-mediated transport	−1.20	0.045
A0A0K9Q4S5	Naringenin-chalcone synthase	flavonoid biosynthetic process	−1.30	0.035
A0A0K9Q3C3	Photosystem I reaction center subunit III	photosynthesis	−1.40	0
A0A0K9PLN1	Eukaryotic translation initiation factor 3	translation	−1.40	0.023
A0A0K9PMD0	50S ribosomal protein L14	translation	−1.60	0.014
A0A0K9P1R8	Serine hydroxymethyltransferase	glycine biosynthetic process from serine	−1.60	0.035
A0A0K9P0D4	Putative 60S ribosomal protein L3	translation	−1.60	0.023
A0A0K9PCA3	7-hydroxymethyl chlorophyll a reductase	chlorophyll cycle	−1.60	0.019
A0A0K9Q607	T-complex protein 1 subunit eta	protein folding	−1.70	0.024
A0A0K9P7E4	Putative Calcium lipid binding protein	lipid transport	−1.80	0.009
A0A0K9PHQ1	Actin−97	actin cytoskeleton organization	−2.10	0.022
A0A0K9Q5N4	Actin	actin cytoskeleton organization	−2.20	0.019
A0A0K9Q607	T-complex protein 1 subunit eta	protein folding	−2.30	0.002
A0A0K9Q3I3	phosphoenolpyruvate carboxylase	carbon fixation	−2.50	0.01
A0A0K9PSH1	Mitochondrial phosphate carrier protein	mitochondrial phosphate ion transport	−2.80	0.019
A0A0K9P894	Malate dehydrogenase	tricarboxylic acid cycle	−4.30	0.023
A0A0K9NYC2	Glyceraldehyde−3-phosphate dehydrogenase	glycolytic process	−27.80	0
A0A0K9PLX2	TFIIS central domain-containing protein	DNA-templated transcription	−29.70	0.02

† negative value indicates depletion, positive value indicates accumulation of a protein; *$p \leq 0{,}05$ as threshold for statistical significance.

responsive protein namely thioredoxin-dependent peroxiredoxin and CBS domain-containing protein CBSX3, involved in cellular redox homeostasis together with mitochondrial phosphorylation and membrane electron transport were stimulated. Enrichment of proline, glycine, and fatty acids aligned with a signature indicative of stress response (Table 2). CYN treatment resulted in the inhibition of fatty acid, alkaloids biosynthesis and down regulation of the UDP-N-acetylmuramate dehydrogenase, and lipid calcium-mediated transport proteins belonging to the lignin metabolism. Plasma membrane ATPase depleted as also nitrogen compounds transport within mitochondrial membranes. CYN negatively affected the arginine and serine biosynthesis, led to alteration in protein translation. The semantic representation of the main GO biological processes affected by CAU or by CYN treatments are reported in the Fig. 9.

4. Discussion

The CAU and CYN treatments resulted in a significant reduction in leaf growth among *P. oceanica* genets. CYN exhibited the most pronounced impact on the mortality of adult leaves and the growth of surviving ones. It also seemed to impede the generation of new leaves, potentially by influencing cell division in the apical meristem of shoots. Although intermediate leaves managed to survive the treatment, their growth rate decreased, leading to an overall reduction in leaf longevity.

These findings are consistent with observations in natural habitats where *P. oceanica* meadows competed with *C. taxifolia* (Pergent et al., 2008) and *C. cylindracea* (Bernardeau-Esteller et al., 2020). In response to competitive interactions with *C. taxifolia*, *P. oceanica* experienced reduced shoot density and leaf length, accompanied by decreased leaf longevity and an increase in leaf growth rate per year (Molenaar et al., 2009; Pergent et al., 2008). Conversely, *C. taxifolia* was found to increase frond length while decreasing the content of CYN (Pergent et al., 2008). In meadows invaded by *C. cylindracea*, *P. oceanica* populations displayed stable or progressive trends, with no discernible structural differences between invaded and non-invaded meadows (Bernardeau-Esteller et al., 2020). This suggests the presence of limiting

Table 2
Proteins that showed high variations in expression in leaves after the caulerpenyne (CYN) treatment are reported. The accession number, protein name, associated GO biological process, fold change (FC) expressed as Log_2 compared to reference, and statistical significance are provided.

Accession	Protein names	Biological Process	FC (Log_2)†	T-test *p*value*
A0A0K9P0Y6	Uridine kinase	de novo' pyrimidine biosynthetic process	3.7	0.019
A0A0K9PNE7	Pleiotropic drug resistance protein 3	abscisic acid transport	3.5	0.029
A0A0K9NRH5	DCD domain-containing protein	response to endoplasmic reticulum stress	2.9	0.034
A0A0K9PPR2	geranylgeranyl diphosphate reductase	chlorophyll biosynthetic process	2.4	0.032
A0A0K9PWX4	Actin−11	cell expansion	2.4	0.05
A0A0K9Q5N4	Actin	actin cytoskeleton organization	2.4	0.003
A0A0K9PDJ3	CBS domain-containing protein CBSX3, mitochondrial	cell redox homeostasis	2.3	0.047
A0A0K9Q3H5	V-type proton ATPase catalytic subunit A	proton transmembrane transport	2.2	0.017
A0A0K9P513	Phosphoglycerate kinase	glycolytic process	2.1	0.004
A0A0K9P0W0	ATP synthase subunit beta	H+ motive force-driven mitochondrial ATP synthesis	2	0.042
A0A0K9PYJ1	Actin-85C	actin cytoskeleton organization	1.8	0.003
A0A0K9NXB5	aldo-keto reductase 2	monoatomic ion transmembrane transport	1.7	0.002
A0A0K9Q5N4	Actin	actin cytoskeleton organization	1.6	0.001
A0A0K9PDL5	ADP-ribosylation factor family protein	ER to Golgi vesicle-mediated transport	1.5	0.006
A0A0K9Q477	proline–tRNA ligase	prolyl-tRNA aminoacylation	1.3	0.008
A0A0K9NWF9	Biotin carboxylase	fatty acid biosynthetic process	1.3	0.038
A0A0K9PK03	30S ribosomal protein S9	translation	1.2	0.031
A0A0K9PXF2	26S proteasome non-ATPase regulatory subunit 1 homolog	proteolysis	1.1	0.011
A0A0K9NTT8	Adenosine kinase (AK)	AMP salvage	1.1	0.007
A0A0K9NU31	Succinate dehydrogenase [ubiquinone] flavoprotein subunit	mitochondrial electron transport	1.1	0.017
A0A0K9P1N1	malate dehydrogenase (NADP(+))	tricarboxylic acid cycle	1.1	0.035
A0A0K9PMD0	50S ribosomal protein L14	translation	1.1	0.03
A0A0K9PLF0	Serine hydroxymethyltransferase	glycine biosynthetic process from serine	1.1	0.013
A0A0K9PDL7	thioredoxin-dependent peroxiredoxin	cell redox homeostasis	1	0.004
A0A0K9Q3I9	Citrate synthase	tricarboxylic acid cycle	1	0.026
A0A0K9Q2H9	phosphoglucomutase	glucose metabolic process	1	0.007
A0A0K9NJ48	fumarate hydratase	tricarboxylic acid cycle	1	0.023
A0A0K9P316	DUF642 domain-containing protein	photosynthetic electron transport chain	−1	0.024
A0A0K9NN51	Glyceraldehyde−3-phosphate dehydrogenase	glycolytic process	−1	0.037
A0A0K9P1G7	Pantothenate kinase 2	coenzyme A biosynthetic process	−1.1	0.029
A0A0K9PFE3	Plasma membrane ATPase	regulation of intracellular pH	−1.1	0.008
A0A0K9PPL3	40S ribosomal protein S19–3	translation	−1.1	0.04
A0A0K9NZM1	trans-cinnamate 4-monooxygenase	lignin metabolic process	−1.1	0.017
A0A0K9P7E4	Putative Calcium lipid binding protein	lipid transport	−1.2	0.049
A0A0K9PTC5	ATP-dependent 6-phosphofructokinase (ATP-PFK)	fructose 6-phosphate metabolic process	−1.3	0.041
A0A0K9PXE8	Fructose-bisphosphate aldolase	glycolytic process	−1.3	0.038
A0A0K9PW16	Chlorophyll a-b binding protein, chloroplastic	photosynthesis	−1.5	0.033
A0A0K9P0D4	Putative 60S ribosomal protein L3	translation	−1.6	0.022
A0A0K9PQ40	Ferredoxin–NADP reductase, chloroplastic	photosynthesis	−1.6	0.04
A0A0K9PW16	Chlorophyll a-b binding protein, chloroplastic	photosynthesis	−1.7	0.048
A0A0K9PC51	RuBisCO large subunit-binding protein subunit beta	Protein refolding	−1.7	0.018
A0A0K9Q2E4	D−3-phosphoglycerate dehydrogenase	L-serine biosynthetic process	−1.8	0.027
A0A0K9Q369	transketolase	pentose-phosphate shunt	−1.8	0.037
A0A0K9Q411	UDP-N-acetylmuramate dehydrogenase	alkaloid metabolic process	−1.8	0.036
A0A0K9P3Z2	ATP-dependent 6-phosphofructokinase (ATP-PFK)	fructose 6-phosphate metabolism	−1.8	0.008
A0A0K9NW74	Pyruvate kinase	glycolytic process	−1.9	0.021
A0A0K9PSH1	Mitochondrial phosphate carrier protein	nitrogen compound transport	−2	0.015
A0A0K9PW97	Elongation factor 1-gamma 2	response to chemical/glytation transferase	−2	0.002
A0A0K9PAG1	Lipoxygenase	fatty acid biosynthetic process	−2.1	0.003
A0A0K9PXE8	Fructose-bisphosphate aldolase	glycolytic process	−2.2	0.042
A0A0K9P988	Acetylglutamate kinase	arginine biosynthetic process	−2.3	0.015
A0A0K9NQM5	ATP-dependent zinc metalloprotease FtsH 4	proteolysis	−2.3	0.023
A0A0K9P1N6	Histone H2B	nucleosome assembly	−2.3	0.009
A0A0K9P4Z1	Glyceraldehyde−3-phosphate dehydrogenase	glycolytic process	−2.5	0.001
A0A0K9Q3M9	beta-ketoacyl-[acyl-carrier-protein] synthase I	fatty acid biosynthetic process	−3	0.029
A0A0K9P6L8	Aminotransferase	biosynthetic process	−3.2	0.041
A0A0K9PLX2	TFIIS central domain-containing protein	DNA-templated transcription	−27.1	0.02

† negative value indicates depletion, positive value indicates accumulation of a protein; *$p \leq 0{,}05$ as threshold for statistical significance.

factors for algae growth and survival within intact canopies of the seagrass.

Similarly, the genet treated with CAU exhibited no impact on shoot meristem activity, leaf renewal, or leaf longevity compared to untreated counterparts. Despite the absence of evidence indicating the release of these chemical compounds toward neighboring seagrass (Marbà et al., 2005), the results underscore the potential allelopathic role of CAU and caulerpenye in the competition between *Caulerpa spp* and *P. oceanica* (Defranoux and Mollo, 2020; Mollo et al., 2015; 2023). The question of whether these molecules could be actively released or accumulate in sediments remains unanswered. Regardless of the mechanism, our manipulative trial demonstrated the capacity of exogenous molecules to translocate along the rhizome, reaching the leaf blades where they exert their effects.

Taking a similar route, CYN might mediate the adverse phytotoxicity exerted by *C. taxifolia*, while CAU could contribute to the molecular inter-specific competition that leads to resilient plants in areas invaded by *C. cylindracea* within *P. oceanica*. This ultimately influences the distinctive invasive capabilities of the two algal species in their natural habitat. However, proposed mechanisms of CYN toxicity towards *P. oceanica* encompass oxidative stress, cytogenetic toxicity, and interference with the photosynthetic process by disrupting chloroplast

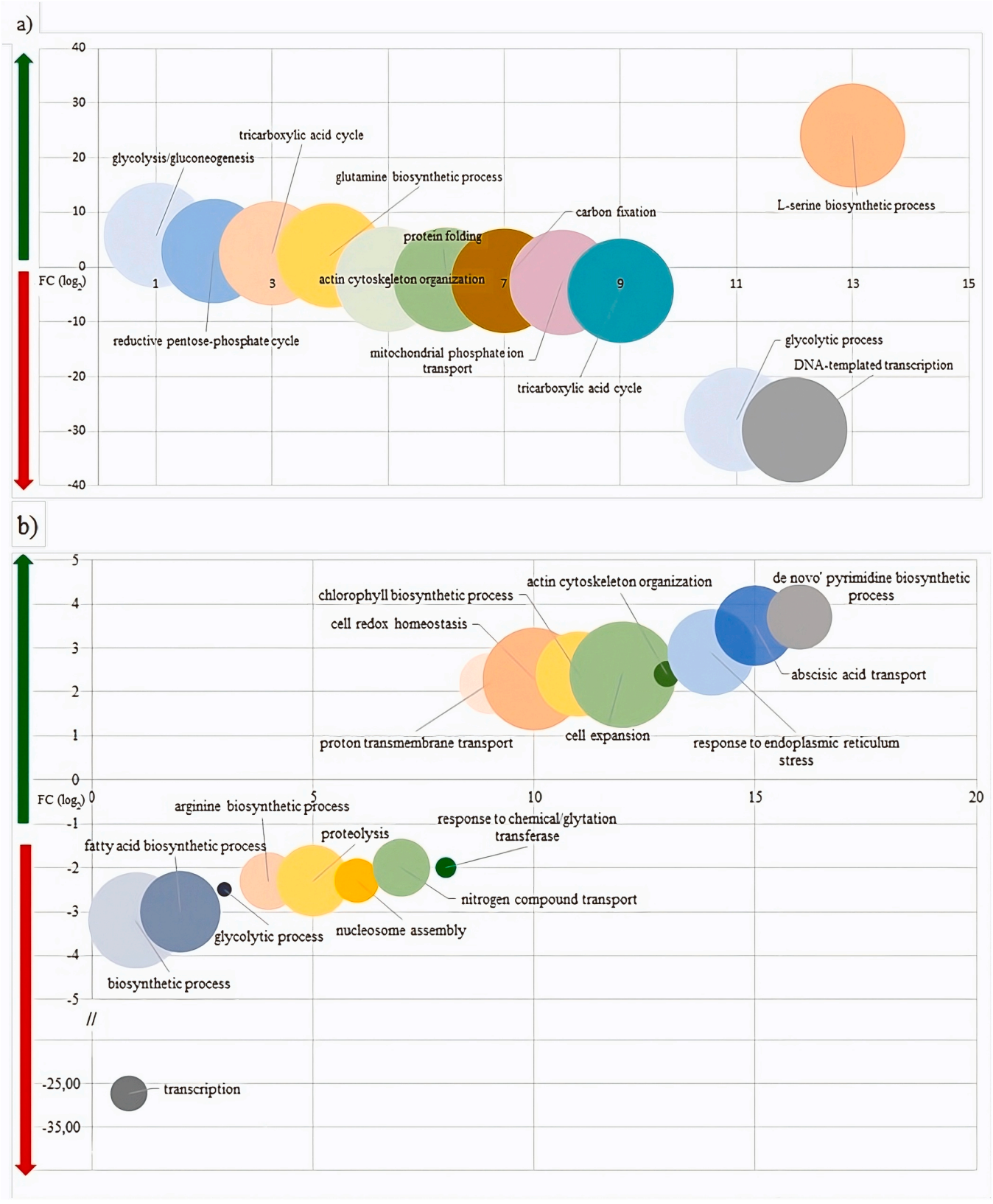

Fig. 9. Semantic representation sorted by Fold changes (Log_2FC) of -DAPs belonging to the main GO biological processes in caulerpenyne (a) or in caulerpin (b) treatments from *Posidonia oceanica* genets. The details of the analysis are reported in the Supplementary Tables 1.

function or inhibiting the biosynthesis of photosynthetic pigments. This disruption ultimately leads to reduced energy production and impaired growth; in algae, this chemical compound is extensively accumulated and serves various functions, including defense mechanisms and participation in signaling pathways (Dumay et al., 2002a, 2002b). Previous experiment using metabolites from *C. cylindracea* applied onto leaf fragments of the *Cymodocea nodosa*, demonstrated that, only CYN had toxicity toward the photosynthetic apparatus of plant, even at exceedingly low concentrations (Raniello et al., 2007). At nuclear level, we found that CYN disrupted chromatin structures and altered the efficiency of mRNA synthesis. The RNA polymerase II elongation cofactor TFIIS (transcription factor IIS) enables transcriptional synthesis within the chromatin context; nucleosomes, indeed, are the main obstacles to efficient elongation (Antosz et al., 2020). The drastic reduction of this enzyme associated with that of histone H2B and accumulation of Uridine kinase, suggests that CYN disrupted the correct transcriptional output and altered the nucleotide biosynthesis, influencing proper leaf growth and development. At cytoplasm level, reorganization of the cytoskeleton and increasing vacuole acidification aligned with promotion of cell elongation instead cell division by the treatment. Several actin proteins were accumulated and particularly the actin 11 that is related to cell expansion during cell cycle as in response to stress (Huang et al., 1997). The induction of vesicular trafficking within the endoplasmic reticulum, the modulation of transporter proteins on organelle membranes, and the inhibition of lipid transport indicated that CYN interacts with trafficking pathways, thereby altering the dynamic interactions between organelles at the membrane level. At mitochondrial level, CYN impacted redox homeostasis by stimulating the CBS domain-containing protein CBSX3 and thioredoxin-dependent peroxiredoxin. CBSXn are a class of proteins that modulate lignin deposition by controlling H_2O_2 levels and trigger the activation of thioredoxins, thereby bolstering their enzymatic activity to sustain cellular homeostasis during stressful conditions (Yoo et al., 2011). Finally, CYN highly impacted the key enzymes belonging the energy metabolism related to glucose, inhibiting cellular growth. Fatty acid biosynthesis and glycine betaine biosynthesis were induced to cope with energy deficiencies and maintain cellular homeostasis (Salam et al., 2023).

P. oceanica responded efficiently to stress imposed by CAU; L-serine biosynthesis was hugely promoted leading to plants displaying better resilience. Enhanced serine triggered the synthesis of amino acids like glycine, methionine, cysteine, and glutamine, concurring to maintain cellular homeostasis; glycine and glutamine are involved in the nitrogen metabolism, while cysteine can accumulate in response to sulfur availability (Tzin and Galili, 2010; Ros et al., 2014). L-methionine accumulation regulate the ethylene pathway in tomato, and reduced ROS by activating genes encoding ROS scavengers (Feng et al., 2024). CAU also affected carbohydrate metabolism; the significant reduction in glyceraldehyde-3-phosphate dehydrogenase (cGAPDH) levels may be linked to oxidative stress, characterized by an imbalance between reactive oxygen species (ROS) production and antioxidant defense mechanisms. This oxidative stress causes modifications to cGAPDH, leading to its degradation and a substantial decrease in enzyme levels (Purev al., 2008; Zeng et al., 2015). Photosystems I and II and chlorophyll biosynthesis depletion indicated that CAU affected the stability of photosynthetic proteins in chloroplasts, also positively regulated the chlorophyl degradation (Liu et al., 2021).

At cytoplasm level, CAU exerted opposite effects than CYN; it hindered intracellular protein and lipid transport, reduced organization of the tubular network of the endoplasmic reticulum and inhibited mitochondrial phosphate ion transmembrane transport via the mitochondrial phosphate transporter. Transmembrane transport and vesicle-mediated transport represented by the Ras-related protein RABB1c was depleted. RAB GTPases are pivotal proteins that regulate multiple facets of membrane traffic, thus exerting a significant influence on diverse cellular functions and responses. Recent studies suggest that RAB proteins play crucial roles in intracellular trafficking and in mitigate biotic and abiotic stress damages (Tripathy et al., 2021). All these metabolic responses were accompanied by changes in membrane potential and disrupted osmoregulation, highlighting the need for precise coordination of ion transport across both the plasma membrane and the vacuolar membrane, which are equipped with distinct sets of transporter proteins (Li et al., 2024). This coincided with decreased levels of actins due to its accelerated turnover and depolymerization process (Sun et al., 2023).

CAU, similar to CYN, exerted a significant impact on nuclear metabolism, leading to a notable decrease in the levels of TFIIS and histones, with the former experiencing a particularly dramatic reduction. The absence of TFSII has been linked to cell death or associated with seed dormancy in *Arabidopsis thaliana* (Mortensen and Grasser, 2014), whereas its overexpression has been found to confer cells with enhanced tolerance to heat stress (Szádeczky-Kardoss et al., 2022; Obermeyer et al., 2023). Interestingly, even in *A. thaliana*, the destabilization of transcript elongation has been associated with the phenomenon of rapid recovery gene down-regulation (RRGD) following stress (Smith et al., 2024; Yeung et al., 2018).

If such a phenomenon were to occur, it could suggest an adaptive response to stress induced by CAU, aligning with the observed phenological parameters in resilient *P. oceanica* genets.

In this context, it should be of great interest to investigate whether the response toward two molecules differs between the apical and vertical shoot types along the rhizome. In fact, recent studies have demonstrated that there is a functional hierarchy between apical and vertical shoots in response to environmental stress (Ruocco et al., 2021). The authors suggest that the response of vertical shoots supports the survival of apical shoots, which are crucial for propagation, population maintenance, and the colonization of new environments. The cytotoxic effects observed in apical meristems, especially after treatment with CYN, could have implications for spatial propagation of clone, while those in vertical meristems might impact the photosynthetic metabolism.

5. Conclusion

The exogenous application of CAU and CYN, metabolites from *C. cylindracea* and *C. taxifolia*, respectively, resulted in suppressed leaf growth among *P. oceanica* genets. CYN exhibited marked phytotoxicity, hindering new leaf formation and causing mortality in adult leaves. In contrast, CAU showed no noticeable impact on the normal regeneration or lifespan of leaves. Proteomic analysis revealed substantial disruptions at the nuclear level, including transcriptional interference and changes in chromatin organization. Despite the significant disturbance, *P. oceanica* displayed a more efficient response to stress induced by CAU. This response stimulated the biosynthesis of essential amino acids, ensuring cellular homeostasis and mitigating damage associated with reactive oxygen species (ROS). Conversely, plants experienced notable stress in response to CYN, which specifically targeted the apical meristems responsible for clone growth and propagation.

Further investigation is needed to ascertain whether the response to CYN varies based on the type of ramets along the rhizome. Overall, these findings closely align with observations in natural habitats where *P. oceanica* meadows were invaded by either *C. taxifolia* or *C. cylindracea*, emphasizing the significant role of these metabolites in specific allelopathic interactions.

Declarations

On behalf of all authors, the corresponding author states that there is no conflict of interest. The authors declare that they have no competing interests in the publication of this research.

Funding

This research was supported by University of Calabria PhD programmes 36th cycles Academic year 2020-2021, funding from Calabria Regional Operation Program (PON) FSE/FESR 2014–2020 (CCI2014IT16M2OP006), which had no role in the design, execution, interpretation, or writing of the study.

CRediT authorship contribution statement

Silvia Mazzuca: Writing – original draft, Resources, Data curation, Conceptualization. **Dante Matteo Nisticò:** Investigation, Formal analysis. **Manoj Kumar:** Validation, Formal analysis. **Faustino Scarcelli:** Methodology, Investigation. **Marianna Carbone:** Validation, Methodology. **Ernesto Mollo:** Writing – review & editing, Writing – original draft, Conceptualization. **Daniela Oliva:** Validation, Methodology, Investigation, Formal analysis. **Amalia Piro:** Validation, Methodology, Investigation, Data curation.

Declaration of Competing Interest

The authors declare that they have no known competing financial interests or personal relationships that could have appeared to influence the work reported in this paper.

Appendix A. Supporting information

Supplementary data associated with this article can be found in the online version at doi:10.1016/j.envexpbot.2024.105987.

References

Amico, V., Oriente, G., Piattelli, M., Tringali, C., Fattorusso, E., Magno, S., Mayol, L., 1978. Caulerpenyne, an unusual sequiterpenoid from the green alga Caulerpa prolifera. Tetrahedron Lett. 19 (38), 3593–3596. https://doi.org/10.1016/S0040-4039(01)95003-8.

Anjaneyulu, A.S.R., Prakash, C.V.S., Mallavadhani, U.V., 1991. Two caulerpin analogues and a sesquiterpene from Caulerpa racemosa. Phytochemistry 30, 3041–3042.

Antosz, W., Deforges, J., Begcy, K., Bruckmann, A., Poirier, Y., Dresselhaus, T., Grasser, K.D., 2020. *Critical Role of Transcript Cleavage in Arabidopsis RNA Polymerase II Transcriptional Elongation*. Plant Cell 32 (5), 1449–1463. https://doi.org/10.1105/tpc.19.00891.

Bernardeau-Esteller, J., Marín-Guirao, L., Sandoval-Gil, J.M., García-Muñoz, R., Ramos-Segura, A., Ruiz, J.M., 2020. *Evidence for the long-term resistance of Posidonia oceanica meadows to Caulerpa cylindracea invasion*. Aquat. Bot. 160, 103167. https://doi.org/10.1016/j.aquabot.2019.103167.

Bradford, M.M., 1976. *A rapid and sensitive method for the quantitation of microgram quantities of protein utilizing the principle of protein-dye binding*. Anal. Biochem. 72, 248–254. https://doi.org/10.1016/0003-2697(76)90527-3.

Buia, M.C., Zupo, V., Mazzella, L., 1992. Primary production and growth dynamics in *Posidonia oceanica*. Marine Ecol. 13 (1), 2–16. https://doi.org/10.1111/j.1439-0485.1992.tb00336.x.

Cantasano, N., Pellicone, G., Di Martino, V., 2017. The spread of Caulerpa cylindracea in Calabria (Italy) and the effects of shipping activities. Ocean Coast. Manag. 144, 51–58. https://doi.org/10.1016/j.ocecoaman.2017.04.014.

Carbone, M., Gavagnin, M., Mollo, E., Bidello, M., Roussis, V., Cimino, G., 2008. Further syphonosides from the sea hare Syphonota geographica and the sea-grass Halophila stipulacea. Tetrahedron 64 (1), 191–196. https://doi.org/10.1016/j.tet.2007.10.071.

Ceccherelli, G., Cinelli, F., 1999. The role of vegetative fragmentation in dispersal of the invasive alga Caulerpa taxifolia in the Mediterranean. Mar. Ecol. Prog. Ser. 182, 299–303 http://www.jstor.org/stable/24852140.

Ceccherelli, G., Piazzi, L., Balata, D., 2002. Spread of introduced Caulerpa species in macroalgal habitats. J. Exp. Mar. Biol. Ecol. 280 (1–2), 1–11. https://doi.org/10.1016/S0022-0981(02)00336-2.

Chay, C., Cansino, R., Pinzón, C., Torres-Ochoa, R., Martínez, R., 2014. Synthesis and anti-tuberculosis activity of the marine natural product caulerpin and its analogues. Mar. Drugs 12, 1757–1772.

Chisholm, J.R.M., Jaubert, J.M., Giaccone, G., 1996. *Caulerpa taxifolia in the northwest Mediterranean: introduced species or migrant from the Red Sea?* Oceanogr. Lit. Rev. 7 (43), 706–707. https://doi.org/10.1023/A:1014549500678.

Defranoux, F., Mollo, E., 2020. Molecular interactions as drivers of changes in marine ecosystems. Ref. Ser. Phytochem. 121–133. https://doi.org/10.1007/978-3-319-96397-6_64.

Delgado, O., Rodríguez-Prieto, C., Gacia, E., Ballesteros, E. *Lack of severe nutrient limitation in Caulerpa taxifolia (Vahl) C. Agardh, an introduced seaweed spreading over the oligotrophic Northwestern Mediterranean*. https://doi.org/10.1515/botm.1996.39.1-6.61.

Dumay, O., Fernandez, C., Pergent, G., 2002a. *Primary production and vegetative cycle in Posidonia oceanica when in competition with the green algae Caulerpa taxifolia and Caulerpa racemosa*. J. Marine Biol. Assoc. UK 82 (3), 379–387.doi. https://doi.org/10.1017/S0025315402005611.

Dumay, O., Pergent, G., Pergent-Martini, C., Amade, P., 2002b. *Variations in caulerpenyne contents in Caulerpa taxifolia and Caulerpa racemosa*. J. chem. Ecol. 28, 343–352. https://doi.org/10.1023/A:1017938225559.

Feng, L., Li, Q., Zhou, D., Jia, M., Liu, Z., Hou, Z., et al., 2024. B. subtilis CNBG-PGPR-1 induces methionine to regulate ethylene pathway and ROS scavenging for improving salt tolerance of tomato. Plant J. 117 (1), 193–211. https://doi.org/10.1111/tpj.16489.

Hiscox, J.D., 1979. *A method for the extraction of chlorophyll from leaf tissue without maceration*. Canadian j. bot. 57 (12), 1332–1334.

Holmer, M., Marbà, N., Lamote, M., Duarte, C.M., 2009. Deterioration of sediment quality in seagrass meadows (Posidonia oceanica) invaded by macroalgae (Caulerpa sp.). Estuar. Coasts 32, 456–466.

Huang, S., An, Y.Q., McDowell, J.M., McKinney, E.C., Meagher, R.B., 1997. The Arabidopsis ACT11 actin gene is strongly expressed in tissues of the emerging inflorescence, pollen, and developing ovules. Plant Mol. Biol. 33 (1), 125–139. https://doi.org/10.1023/a:1005741514764. PMID: 9037165.

Kanehisa, M., Sato, Y., Morishima, K., 2016. BlastKOALA and GhostKOALA: KEGG tools for functional characterization of genome and metagenome sequences. J. Mol. Biol. 428, 726–731. https://doi.org/10.1016/j.jmb.2015.11.006.

Kolar, C.S., Lodge, D.M., 2001. Progress in invasion biology: predicting invaders. Trends Ecol. Evol. 16 (4), 199–204. https://doi.org/10.1016/s0169-5347(01)02101-2. PMID: 11245943.

Laemli, U.K., 1970. *Cleavage of Structural Proteins during the Assembly of the Head of Bacteriophage T4*. Nat. 227, 680–685. https://doi.org/10.1038/227680a0.

Li, K., Grauschopf, C., Hedrich, R., Dreyer, I., Konrad, K.R., 2024. K^+ and pH homeostasis in plant cells is controlled by a synchronized K^+/H^+ antiport at the plasma and vacuolar membrane. New Phytol. 241, 1525–1542. https://doi.org/10.1111/nph.19436.

Liu, W., Chen, G., Chen, J., Jahan, M.S., Guo, S., Wang, Y., et al., 2021. Overexpression of 7-hydroxymethyl chlorophyll a reductase from cucumber in tobacco accelerates dark-induced chlorophyll degradation. Plants 10 (9), 1820. https://doi.org/10.3390/plants10091820.

Liu, D., Mao, S., Yu, X., Feng, L., Lai, X., 2012. *Caulerchlorin, a novel chlorinated bisindole alkaloid with antifungal activity from the Chinese green alga Caulerpa racemosa*. Heterocycles 85 (3), 661–666. https://doi.org/10.3987/COM-11-12408.

Marbà, N., Duarte, C.M., Díaz-Almela, E., Terrados, J., Álvarez, E., Martínez, R., Grau, A. M., 2005. *Direct evidence of imbalanced seagrass (Posidonia oceanica) shoot population dynamics in the Spanish Mediterranean*. Estuaries 28, 53–62. https://doi.org/10.1007/BF02732753.

Mazzuca, S., Spadafora, A., Filadoro, D., Vannini, C., Marsoni, M., Cozza, R., Innocenti, A.M., 2009. Seagrass light acclimation: 2-DE protein analysis in Posidonia leaves grown in chronic low light conditions. J. Exp. Marine Biol. Ecol. 374 (2), 113–122. https://doi.org/10.1016/j.jembe.2009.04.010.

Meinesz, A., Boudouresque, C., 1996. *Sur l'origine de Caulerpa taxifolia en Méditerranée*. C R Acad. Sci. Paris. Sci. Vie 319, 603–616. https://doi.org/10.1023/A:1014549500678.

Mi, H., Muruganujan, A., Ebert, D., Huang, X., Thomas, P.D., 2019. PANTHER version 14: more genomes, a new PANTHER GO-slim and improvements in enrichment analysis tools. Nucleic Acids Res. 47 (D1), D419–D426. https://doi.org/10.1093/nar/gky1038.

Molenaar, H., Meinesz, A., Thibaut, T., 2009. *Alterations of the structure of Posidonia oceanica beds due to the introduced alga Caulerpa taxifolia*. Scientia Mar. 73 (2), 329–335. https://doi.org/10.3989/scimar.2009.73n2329.

Mollo, E., Cimino, G., Ghiselin, M.T., 2015. Alien biomolecules: a new challenge for natural product chemists. Biol. Invasions 17, 941–950. https://doi.org/10.1007/s10530-014-0835-6.

Mollo, E., Gavagnin, M., Carbone, M., Castelluccio, F., Pozone, F., Ghiselin, M.T., , 2008. Factors promoting marine invasions: a chemoecological approach. https://doi.org/10.1073/pnas.0709355105.

Mortensen, S.A., Grasser, K.D., 2014. The seed dormancy defect of Arabidopsis mutants lacking the transcript elongation factor TFIIS is caused by reduced expression of the DOG1 gene. FEBS lett. 588 (1), 47–51. https://doi.org/10.1016/j.febslet.2013.10.047.

Motmainna, M., Juraimi, A.S., Ahmad-Hamdani, M.S., Hasan, M., Yeasmin, S., Anwar, M. P., et al., 2023. Allelopathic potential of tropical plants—a review. Agronomy 13 (8), 2063. https://doi.org/10.3390/agronomy13082063.

Obermeyer, S., Stöckl, R., Schnekenburger, T., Kapoor, H., Stempfl, T., Schwartz, U., et al., 2023. TFIIS is crucial during early transcript elongation for transcriptional reprogramming in response to heat stress. J. Mol. Biol. 435 (2), 167917. https://doi.org/10.1016/j.jmb.2022.167917.

Oliva, D., Piro, A., Nisticò, M., Scarcelli, F., Mazzuca, S., 2023. *Seagrass Omics: How to Short the Workflow for Protein Expression Analyses*. Examines Mar. Biol. Oceanogr. 5. https://doi.org/10.31031/EIMBO.2023.05.000618.

Pergent, G., Boudouresque, C.F., Dumay, O., Pergent-Martini, C., Wyllie-Echeverria, S., 2008. *Competition between the invasive macrophyte Caulerpa taxifolia and the seagrass Posidonia oceanica: contrasting strategies*. BMC ecol. 8 (1), 1–13. https://doi.org/10.1186/1472-6785-8-20.

Piazzi, L., Balata, D., Ceccherelli, G., Cinelli, F., 2005. Interactive effect of sedimentation and Caulerpa racemosa var. cylindracea invasion on macroalgal assemblages in the

Mediterranean Sea. Estuar., Coast. Shelf Sci. 64 (2-3), 467–474. https://doi.org/10.1016/j.ecss.2005.03.010.

Piro, A., Bernardo, L., Serra, I.A., Barrote, I., Olivé, I., Costa, M.M., Lucini, L., Santos, R., Mazzuca, S., Silva, J., 2020. *Leaf proteome modulation and cytological features of seagrass Cymodocea nodosa in response to long-term high CO2 exposure in volcanic vents*. Sci. Rep. 10, 22332. https://doi.org/10.1038/s41598-020-78764-7.

Purev, M., Kim, M.K., Samdan, N., et al., 2008. Isolation of a novel fructose-1,6-bisphosphate aldolase gene from Codonopsis lanceolata and analysis of the response of this gene to abiotic stresses. Mol. Biol. 42, 179–186. https://doi.org/10.1134/S0026893308020027.

Raniello, R., Mollo, E., Lorenti, M., Gavagnin, M., Buia, M.C., 2007. Phytotoxic activity of caulerpenyne from the Mediterranean invasive variety of Caulerpa racemosa: a potential allelochemical. Biol. Invasions 9, 361–368. https://doi.org/10.1007/s10530-006-9044-2.

Ros, R., Munoz-Bertomeu, J., Krueger, S., 2014. Serine in plants: biosynthesis, metabolism, and functions. Trends Plant Sci. 19, 564–569. https://doi.org/10.1016/j.tplants.2014.06.003.

Ruocco, M., Entrambasaguas, L., Dattolo, E., Milito, A., Marín-Guirao, L., Procaccini, G., 2021. A king and vassals' tale: molecular signatures of clonal integration in Posidonia oceanica under chronic light shortage. J. Ecol. 109 (1), 294–312.

Russo, T., Coppola, F., Leite, C., Carbone, M., Paris, D., Motta, A., et al., 2023. An alien metabolite vs. a synthetic chemical hazard: an ecotoxicological comparison in the Mediterranean blue mussel. Sci. Total Environ., 164476 https://doi.org/10.1016/j.scitotenv.2023.164476.

Salam, U., Ullah, S., Tang, Z.H., Elateeq, A.A., Khan, Y., Khan, J., Ali, S., 2023. Plant metabolomics: An overview of the role of primary and secondary metabolites against different environmental stress factors. Life 13 (3), 706. https://doi.org/10.3390/life13030706.

Sfecci, E., Le Quemener, C., Lacour, T., Massi, L., Amade, P., Audo, G., et al., 2017. CYN from Caulerpa taxifolia: a comparative study between CPC and classical chromatographic techniques. Phytochem Lett. 20 (2016), 406–409.

Shea, K., Chesson, P., 2002. Community ecology theory as a framework for biological invasions. Trends Ecol. Evol. 17 (4), 170–176. https://doi.org/10.1016/S0169-5347(02)02495-3.

Simberloff, D., Martin, J.L., Genovesi, P., Maris, V., Wardle, D.A., Aronson, J., Vilà, M., 2013. *Impacts of biological invasions: what's what and the way forward*. Trends ecol. evol. 28 (1), 58–66. https://doi.org/10.1016/j.tree.2012.07.013.

Smith, A.B., Ganguly, D.R., Moore, M., Bowerman, A.F., Janapala, Y., Shirokikh, N.E., et al., 2024. Dynamics of mRNA fate during light stress and recovery: from transcription to stability and translation. Plant J. 117 (3), 818–839. https://doi.org/10.1111/tpj.1653.

Streftaris, N., Zenetos, A., 2006. *Alien Marine Species in the Mediterranean - the 100 'Worst Invasives' and their Impact*. Mediterr. Mar. Sci. 7. https://doi.org/10.12681/mms.180.

Sun, Y., Shi, M., Wang, D., Gong, Y., Sha, Q., Lv, P., et al., 2023. Research progress on the roles of actin-depolymerizing factor in plant stress responses. Front. Plant Sci. 14, 1278311. https://doi.org/10.3389/fpls.2023.1278311.

Szádeczky-Kardoss, I., Szaker, H.M., Verma, R., Darkó, É., Pettkó-Szandtner, A., Silhavy, D., et al., 2022. Elongation factor TFIIS is essential for heat stress adaptation in plants. Nucleic Acids Res. 50 (4), 1927–1950. https://doi.org/10.1093/nar/gkac020.

Tripathy, M.K., Deswal, R., Sopory, S.K., 2021. Plant RABs: Role in Development and in Abiotic and Biotic Stress Responses. Curr. Genomics 22 (1), 26–40. https://doi.org/10.2174/1389202922666210114102743.

Tzin, V., Galili, G., 2010. The biosynthetic pathways for shikimate and aromatic amino acids in Arabidopsis thaliana. Arab. Book 8, e0132. https://doi.org/10.1199/table0132.

, 2002Williams, SL, Grosholsz, ED (Eds.), 2002. *Preliminary reports from the Caulerpa taxifolia invasion in southern California*. Ecol Prog Ser 233, 307–310.

Yeung, E., Van Veen, H., Vashisht, D., et al., 2018. A stress recovery signaling network for enhanced flooding tolerance in. Proc. Natl. Acad. Sci. USA 115, E6085–E6094. https://doi.org/10.1073/pnas.1803841115.

Yoo, K.S., Ok, S.H., Jeong, B.C., Jung, K.W., Cui, M.H., Hyoung, S., et al., 2011. Single cystathionine β-synthase domain-containing proteins modulate development by regulating the thioredoxin system in Arabidopsis. Plant Cell 23 (10), 3577–3594. https://doi.org/10.1105/tpc.111.089847.

Zeng, Y., Tan, X., Zhang, L., et al., 2015. A fructose-1,6-biphosphate aldolase gene from *Camellia oleifera*: molecular characterization and impact on salt stress tolerance. Mol. Breeding 35, 17. https://doi.org/10.1007/s11032-015-0233-5.

Zieman, J.C., 1974. Methods for the study of the growth and production of turtle grass, Thalassia testudinum König. Aquaculture 4, 139–143. https://doi.org/10.1016/0044-8486(74)90029-5.

Zubia, M., Draisma, S.G., Morrissey, K.L., Varela-Álvarez, E., De Clerck, O., 2020. Concise review of the genus Caulerpa JV Lamouroux. J. Appl. Phycol. 32, 23–39. https://doi.org/10.1007/s10811-019-01868-9.